Supplementary Material to "Structural Transitions and Thermodynamics of a Glycine-Dependent Riboswitch from *Vibrio cholerae*"

Jan Lipfert[1], Rhiju Das[1,2,3], Vincent B. Chu[4], Madhuri Kudaravalli[2], Nathan Boyd[2], Daniel Herschlag[2], and Sebastian Doniach[1,3,5,⋆]

September 27, 2006

[1]Departments of Physics, [2]Biochemistry, [4]Applied Physics, and [5]Biophysics Program,

Stanford University, Stanford, CA 94305, USA

[3]Current address: Departments of Biochemistry and Genome Sciences,

University of Washington, Seattle, WA 98195, USA

[⋆]Corresponding author

Email address of the corresponding author: doniach@drizzle.stanford.edu

Glycine titration: Two- and three-state fits to the SAXS data

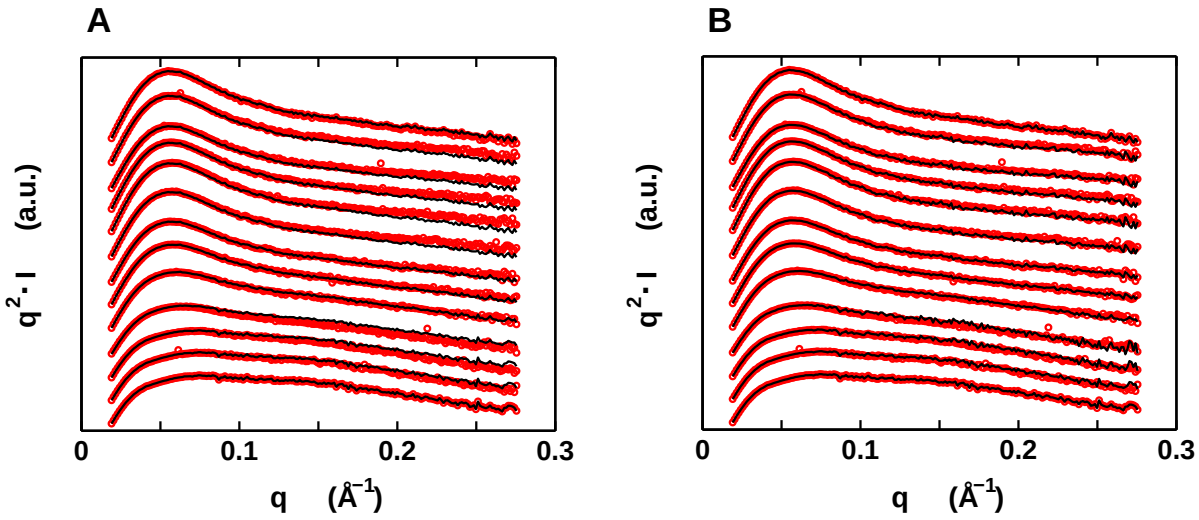

Fig. S1. SAXS profiles in Kratky representation $[q^2 \cdot I(q)$ as a function of $q]$ for different glycine concentrations in the presence of 10 mM Mg^{2+}. Experimental data (red circles) and fitted profiles from two-state projections (A, black lines) and best three-state fit (B, black lines). Glycine concentrations are (from bottom to top profile in both graphs) 0, 10, 20, 50, 100, 200, 500 μM , 1, 2, 5, 10, 20, and 50 mM. The number of points in the experimental profiles was reduced for clarity.

Glycine titration: Hydroxyl radical footprinting

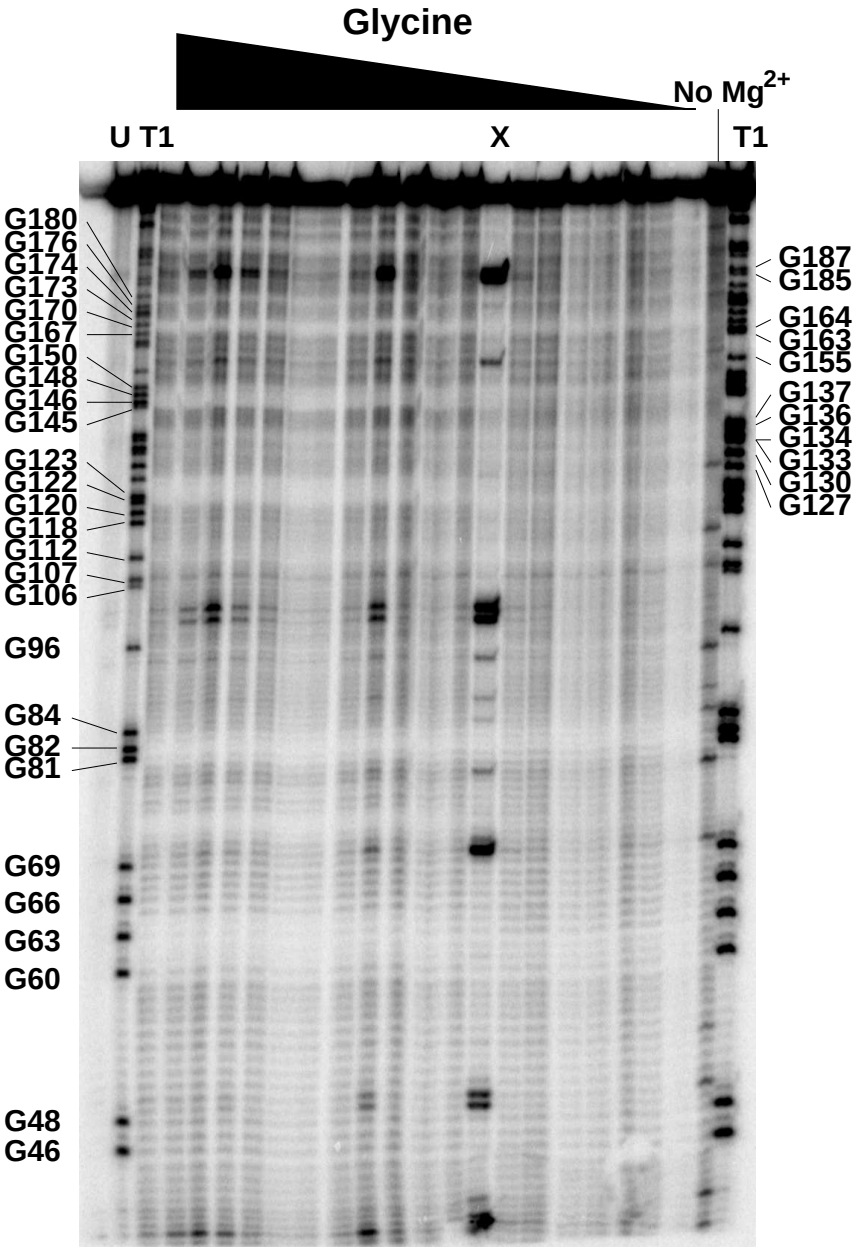

Fig. S2. Example of a gel image of the hydroxyl radical footpriting data as a function of glycine.

Lanes from left to right are: U (untreated, no reaction), T1 (T1 digest), 10 mM $MgCl_2$ and 100, 50, 25, 10, 5, 2.5, 2.5, 1 mM, 500, 250, 100, 50, 25, 10, 5, 2.5, 2.5, 1, 0, 0 μM glycine, No Mg^{2+} (no $MgCl_2$ added), and T1 (T1 digest, repeat). In this gel, the lane with 25 μM glycine (marked with "X" in the figure) was strongly contaminated (presumbaly due to RNAase activity) and excluded from the analysis. The T1 digest ladder is annotated to the left of the figure, for reasons of clarity, three blocks of residues (G127 to G137, G155 to G164, and G185 to G187) are annotated on the right. Footprinting data was extracted from the gel images using the software SAFA, which uses a peak fitting routine. The extracted data was normalized and standardized and data from several gels were averaged (see text). However, protections from cleavage in several regions are visible in the gel image. In particular the protections with increasing glycine concentration around residue G63, around residue 73 (between G69 and G81), around G82, at and above G123, at and above G145, and (faintly) around residue G170.

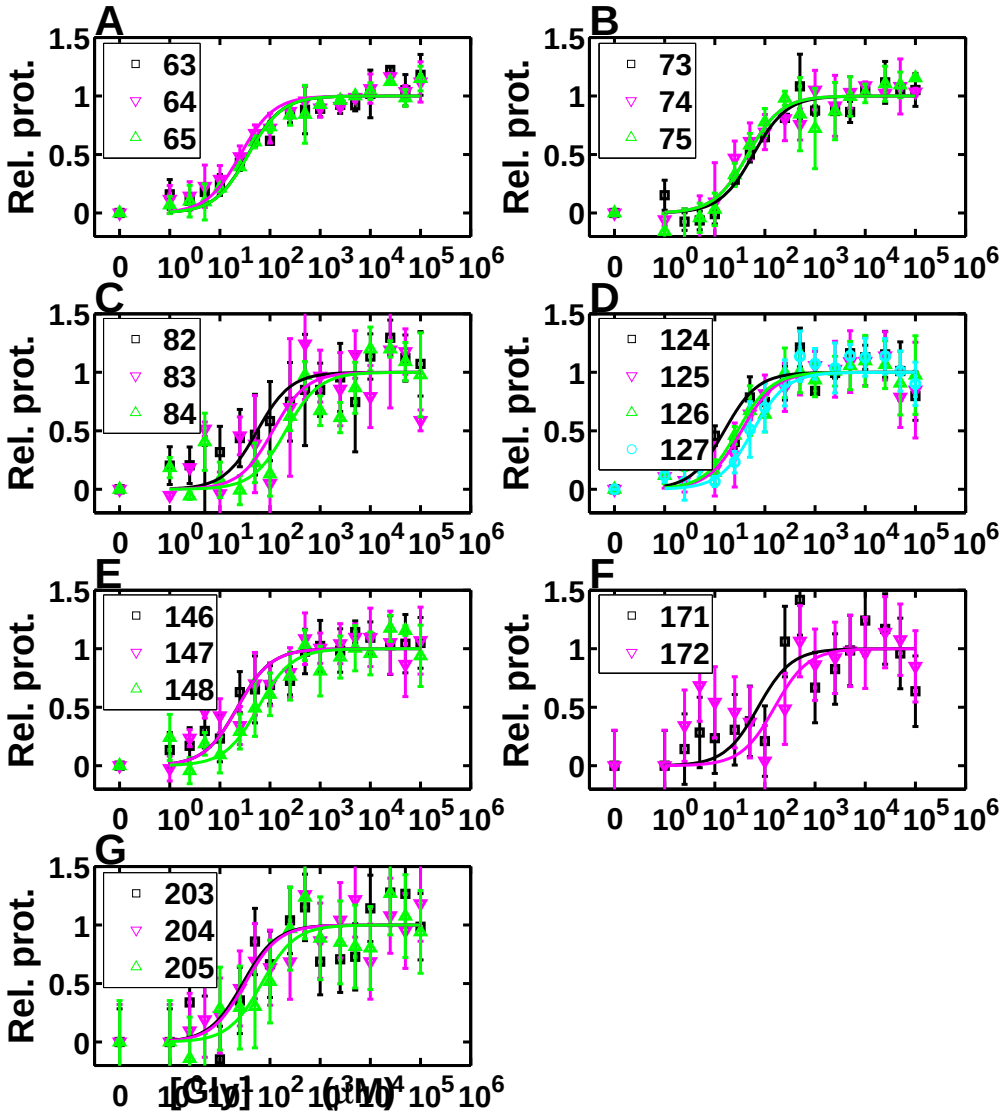

Fig. S3. Relative protections from hydroxyl radical induced cleavage as a function of glycine in the presence of 10 mM Mg^{2+} for the VCI-II riboswitch tandem aptamer. Protections (symbols)

are scaled such that the value in the absence of glycine corresponds to zero, and full protections in 100 mM glycine are normalized to one. Data were fit using the Hill equation with a fixed Hill coefficient of $n = 1.4$ (solid lines). Panels A-G show footprinting data for different regions of the RNA where protections from hydroxyl radical induced cleavage are present, the corresponding residues are shown in the figure insets. Regions in A (residues 63-65), B (residues 73-75), C (residues 82-84) and D (residues 124-127) are located in aptamer I of VCI-II, regions in panel E (residues 146-148), F (residues 171-172) and G (residues 203-205) are located in aptamer II. Data for region A-E correspond to averages and standard deviations from at least triple repeat measurements. The data for regions F and G are from a single measurement and are thus of lower quality. The Hill midpoint values obtained from the fits are presented in Table S1.

Region	Residues	Hill midpoint ($K_{\mathrm{mid,Gly}}$, μM)
A	63-65	33 ± 10
B	73-75	50 ± 10
C	82-84	110 ± 30
D	124-127	35 ± 18
E	146-148	35 ± 21
F	171-172	115 ± 60
G	203-205	42 ± 22

Table S1. Hill midpoints for the hydroxyl radical footprinting data as a function of glycine concentration shown in Figure S3. The regions refer to the sets of residues from Figure S3. Midpoint values were averaged over the different residues from each region. Averaging over all transitions, the midpoint is $K_{\mathrm{mid,Gly}} = 60 \pm 25$ μM glycine. For details of the footprinting experiments and analysis see the main text.

Mg^{2+} titration: SAXS

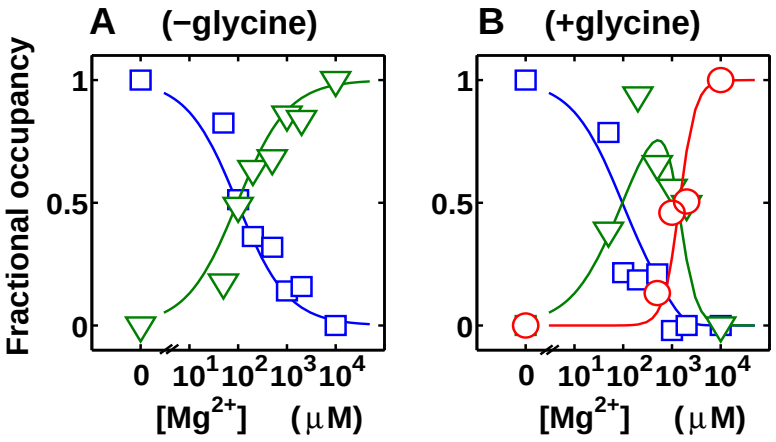

Fig. S4. Two- and three-state projections of the SAXS profiles as a function of magnesium concentration, in the absence of glycine (A, left) and in the presence of 10 mM glycine (B, right). For the Mg^{2+} titration with no glycine added, experimental fractional occupancies were determined for the U (A, blue squares) and M states (A, green triangles) by projecting the full experimental scattering profiles onto the profiles measured in 0 and 10 mM Mg^{2+}, respectively. For the Mg^{2+} titration in the presence of 10 mM glycine, experimental fractional occupancies are obtained for the U (B, blue squares), M (B, green triangles), and B states (B, red circles) by projecting the experimental data onto the scattering profiles measured in 0 and 10 mM Mg^{2+} with no added glycine for the U and M states and that measured in 10 mM glycine and 10 mM Mg^{2+} for the B state. Solid lines are the result of a global fit of the thermodynamic model described in the main text. The parameters for the fit shown are $m_1 = 0.85$, $K_1 = 100$ μM and $m_2 = 2.2$. The size of the symbols was chosen to approximately indicate the size of the errors.

Mg^{2+} titration with no glycine present: Hydroxyl radical footprinting

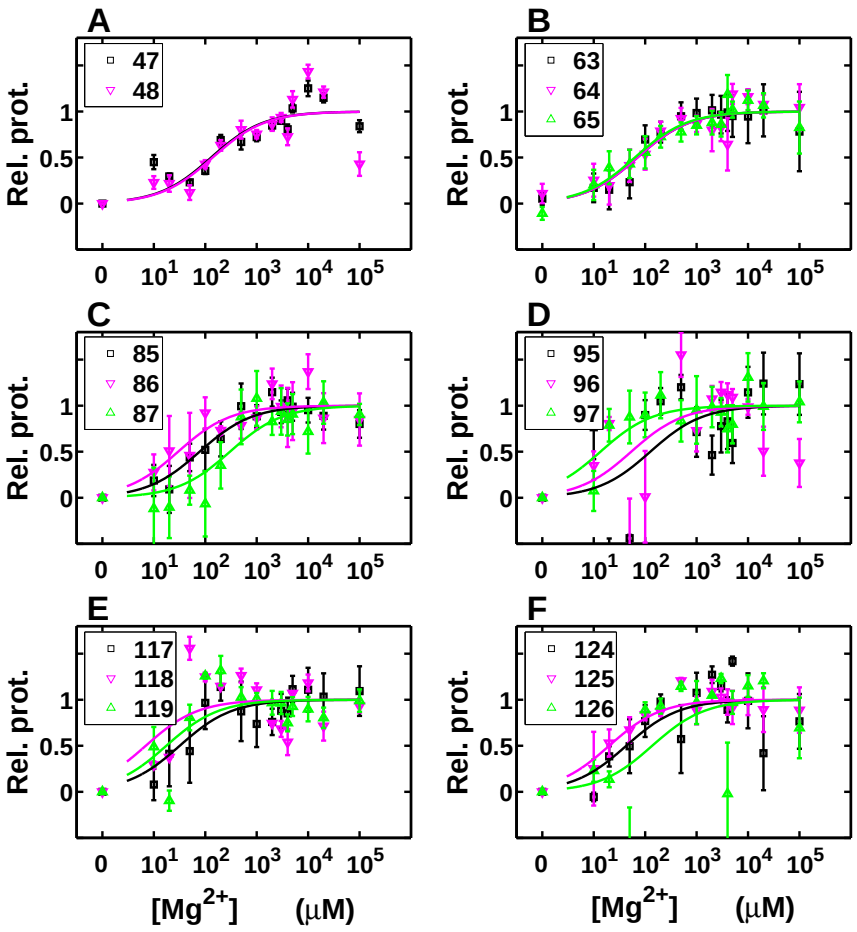

Fig. S5. Relative protections from hydroxyl radical induced cleavage as a function of Mg^{2+} for the VCI-II tandem aptamer with no glycine present. Protections from cleavage (symbols) are scaled such that the value at 0 mM Mg^{2+} corresponds to zero, and full protections in 100 mM Mg^{2+} are normalized to one. Data were fit using the Hill equation with a fixed Hill coefficient of $n = 0.85$ (solid lines). Panels A-F show footprinting data for different regions of the RNA where protections from hydroxyl radical induced cleavage are present, the corresponding residues are shown in the

figure insets. All data correspond to averages and standard deviations from at least triple repeat measurements. The Hill midpoint values obtained from the fit are presented in Table S2.

Region	Residues	Hill midpoint (K_1, μM)
A	47-48	130 ± 20
B	63-65	66 ± 25
C	85-87	261 ± 80
D	95-97	63 ± 45
E	117-119	20 ± 10
F	124-126	64 ± 30

Table S2. Hill midpoints for the hydroxyl radical footprinting data as a function of Mg^{2+} concentration with no added glycine shown in Figure S5. The regions refer to the sets of residues from Figure S5. Midpoint values were averaged over the different residues from each region. For details of the footprinting experiments and analysis see the main text.

Mg^{2+} titration with 10 mM glycine present: Hydroxyl radical footprinting

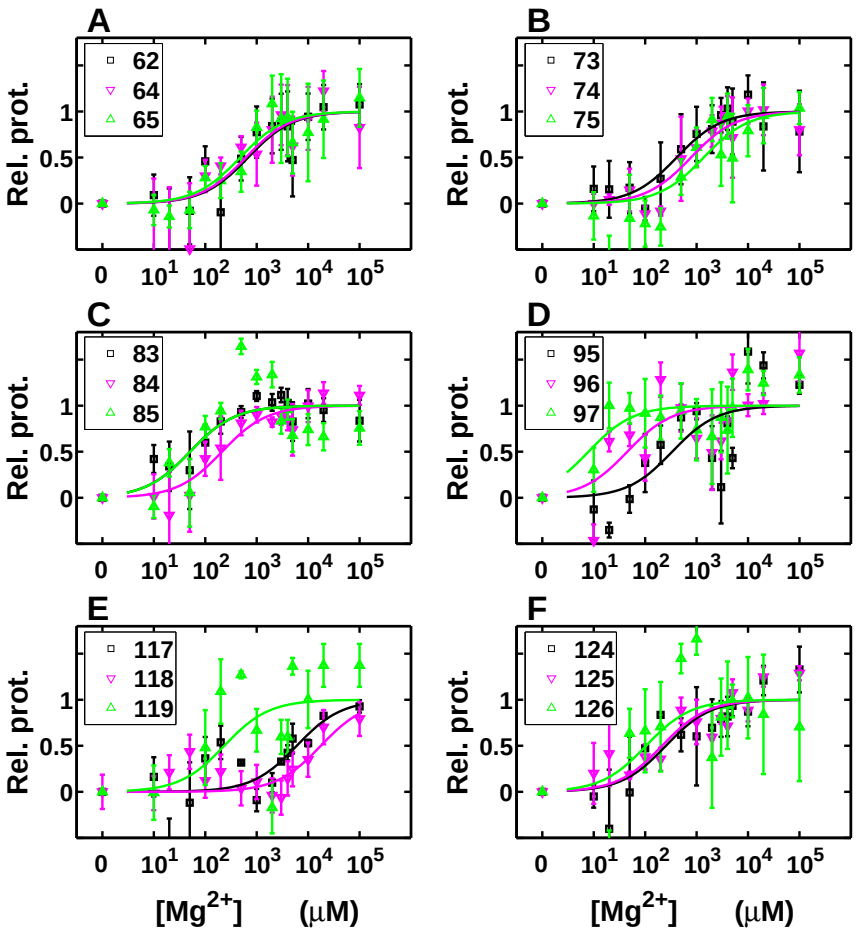

Fig. S6. Relative protections from hydroxyl radical cleavage as a function of Mg^{2+} for the VCI-II construct with 10 mM glycine present. Protections from cleavage (symbols) are scaled such that the value at 0 mM Mg^{2+} corresponds to zero, and full protections in 100 mM magnesium are normalized to one. For simplicity, data were fit using the Hill equation with a fixed Hill coefficient of $n = 1.0$ (solid lines) to obtain apparent midpoints. Panels A-F show footprinting data for different regions of the RNA where protections from hydroxyl radical induced cleavage are present, the corresponding

residues are shown in the figure insets. All data correspond to averages and standard deviations from at least triple repeat measurements. The apparent midpoint values obtained from the fits are presented in Table S3.

Region	Residues	Hill midpoint ($K_{apparent}$, μM)
A	62,64-65	590 ± 100
B	73-75	850 ± 200
C	83-85	100 ± 50
D	95-97	130 ± 50
E	117-119	> 1000
F	124-126	190 ± 70

Table S3. Apparent midpoints for the hydroxyl radical footprinting data as a function of Mg^{2+} concentration with 10 mM glycine added shown in Figure S6. The midpoint values were obtained from two-state Hill fits with a fixed Hill coefficient of $n = 1$ and averaged over the different residues from each region. The regions refer to the sets of residues from Figure S6. For details of the footprinting experiments and analysis see the main text.

Low resolution structures

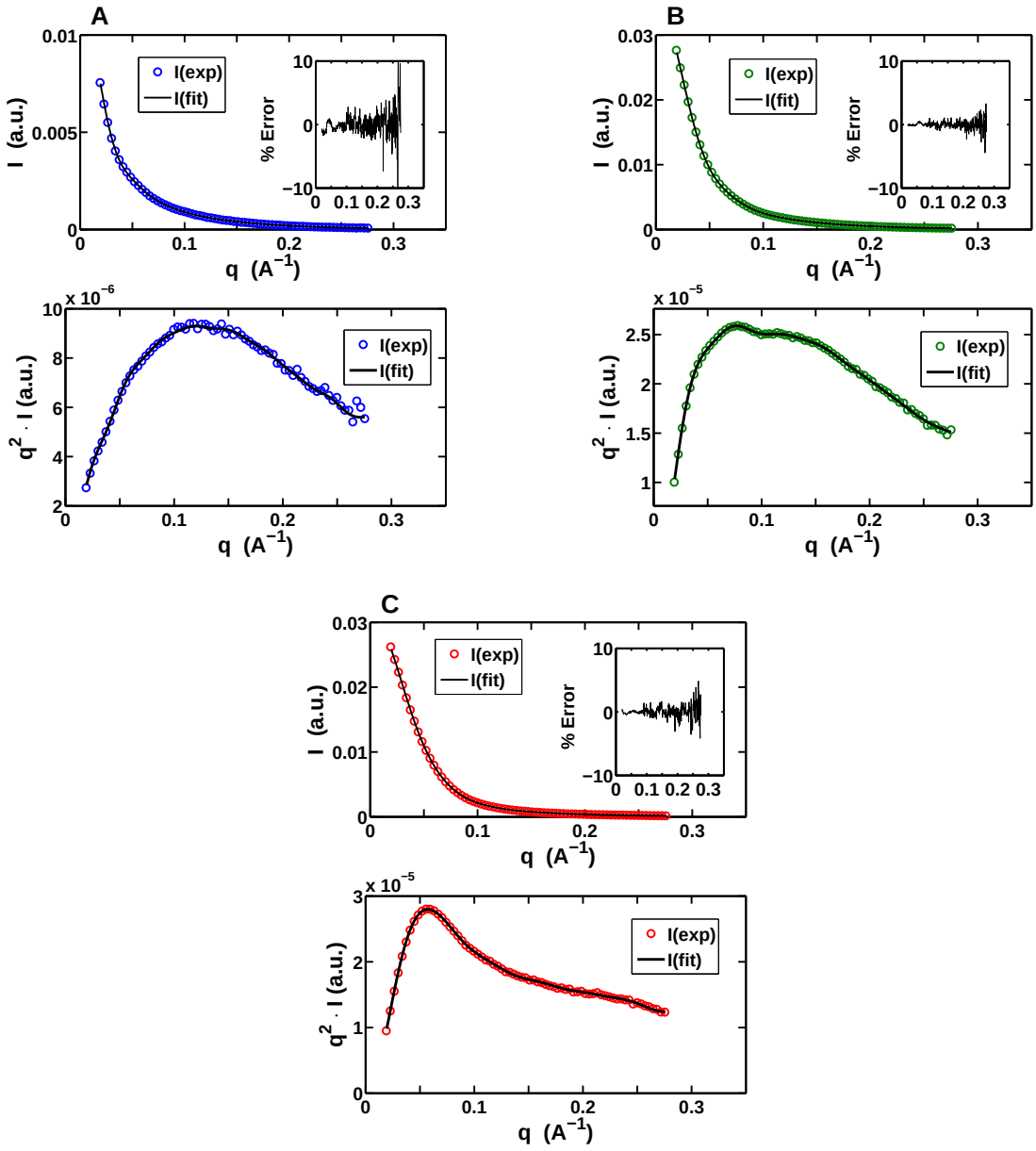

Fig. S7. Experimental scattering profiles (colored circles) for the U (A, blue), M (B, green) and B state (C, red) of the VCI-II riboswitch tandem aptamer and scattering profiles from the

corresponding bead reconstructions (black lines). The top graphs in A, B and C show the profiles as $I(q)$ and the relative error $(I(exp,q)-I(fit,q))/I(exp,q)\cdot 100\%$ in the insets. The bottom graphs in A, B and C show the experimental profile and corresponding bead fits in Kratky representation [$q^2 \cdot I(q)$ as a function of q]. The number of points in the experimental profiles was reduced for clarity; reconstructions used the software dammin.[1] For details of the reconstructions and solution conditions see the main text and Table 2.

References

[1] Svergun, D. I. (1999) Restoring low resolution structure of biological macromolecules from solution scattering using simulated annealing. *Biophys. J.,* **76**, 2879–2886.